

stretch fundamentals (which overlap at 3523 cm^{-1}) produces little net change in the population of the three conformations, consistent with their position remote from the dipeptide backbone.

The observation of vibrational mode-selectivity in the conformational isomerization of a molecule of this size is an unexpected result. Many previous studies on much smaller molecules have concluded that vibrationally mode-specific behavior is increasingly unlikely as the size of the molecule increases (12, 13). Intramolecular vibrational redistribution, or vibrational state mixing, increases with increasing molecular size because the density of vibrational states at a given energy rises quickly with increasing molecular size, washing out mode-specific excitation by diluting the make-up of the state carrying the oscillator strength with an increasing number of background levels at that energy.

However, the present experiment probes conformational isomerization rather than bond breaking, with barriers separating the conformational minima of about 20 kJ/mol, total excitation energies of only about 40 kJ/mol, and fast cooling in the expansion (with the first cooling collision on the 10^{-10} s time scale). Such conditions could limit the extent to which energy can redistribute throughout the molecule before trapping behind a barrier to isomerization. If the molecule is large enough, the parts of the molecule far from the point of excitation should play little role in the dynamics that follow IR excitation. In this sense, vibrational mode-selectivity may be more readily achieved in very large molecules than in small ones, if selective excitation can be achieved. In addition, the cooling collisions may participate in changing the conformational populations rather than simply quenching them. Thus, in the presence of competing deactivation, the kinds of conformational change that can be induced by IR excitation may have a characteristic length scale that the present experiment could be beginning to explore, pointing to the need for further experiments of this kind, supported by theory.

References and Notes

1. V. C. Vachev, J. H. Frederick, B. A. Brishanin, V. N. Zadkov, N. I. Koroteev, *J. Phys. Chem.* **99**, 5247 (1995).
2. F. M. Richards, in *Protein Folding*, T. E. Creighton, Ed. (Freeman, New York, 1992), pp. 1–58.
3. P. N. Mortenson, D. J. Wales, *J. Chem. Phys.* **114**, 6443 (2001).
4. W. D. Cornell, *et al.*, *J. Am. Chem. Soc.* **117**, 5179 (1995).
5. D. Evans, D. J. Wales, personal communication.
6. T. Head-Gordon, M. Head-Gordon, M. J. Frisch, C. L. Brooks III, J. A. Pople, *J. Am. Chem. Soc.* **113**, 5989 (1991).
7. M. J. Tubergen, J. R. Cable, D. H. Levy, *J. Chem. Phys.* **92**, 51 (1990).
8. B. C. Dian, A. Longarte-Aldamo, S. Mercier, T. S. Zwier, in preparation.
9. T. S. Zwier, *J. Phys. Chem. A* **105**, 8827 (2001).

10. These measurements are equivalent to a photochemical quantum yield measurement. Photoexcitation of conformer I produces a certain population of excited molecules. The quantum yield Φ_{ij} is then the fraction of this excited population of conformer I that ends up as conformer J.
11. On the basis of preliminary results from *N*-acetyltryptophan amide and melatonin.
12. D. J. Nesbitt, R. W. Field, *J. Phys. Chem.* **100**, 12735 (1996).

13. F. F. Crim, *J. Phys. Chem.* **100**, 12725 (1996).
14. We acknowledge the National Science Foundation and the Petroleum Research Fund for support of this research (grant CHE-9728636). A.L. acknowledges the MCYT for his postdoctoral fellowship.
Published online 23 May 2002;
10.1126/science.1071563
Include this information when citing this paper.

6 March 2002; accepted 15 May 2002

Nitrate Controls on Iron and Arsenic in an Urban Lake

David B. Senn*† and Harold F. Hemond

Aquatic ecosystems are often contaminated by multiple substances. Nitrate, a common aquatic pollutant, strongly influenced the cycling of arsenic (As) under anoxic conditions in urban Upper Mystic Lake (Massachusetts, USA) by oxidizing ferrous iron [Fe(II)] to produce As-sorbing particulate hydrous ferric oxides and causing the more oxidized As(V), which is more particle-reactive than As(III) under these conditions, to dominate. This process is likely to be important in many natural waters.

Arsenic cycling in aquatic systems is strongly influenced by redox processes. For example, oxidized [arsenate, $\text{H}_2\text{As}^{(\text{V})}\text{O}_4^-$] and reduced [arsenite, $\text{H}_3\text{As}^{(\text{III})}\text{O}_3$] forms of inorganic As can differ both in their tendency to form soluble or insoluble complexes (1–3) and in their toxicity to humans and aquatic communities (1). Moreover, because surface complexation of As by solid hydrous ferric oxide (HFO; Fe in the +III oxidation state) often plays a dominant role in immobilizing As (2, 3), redox processes that affect Fe speciation can also have a strong indirect effect on As (4). Thus, redox-active pollutants (oxidants or reductants) could have the potential to affect As mobility. Nitrogen (N) pollution, arising from activities such as agricultural fertilization and fuel combustion, is generally of concern for its roles in eutrophication and acidification (5); however, nitrate (NO_3^-), one of the major forms of fixed N, is also a powerful oxidant. Laboratory studies have recently identified bacteria that can mediate both Fe(II) (6–8) and As(III) (9) oxidation by NO_3^- , and field evidence suggests that NO_3^- may influence Fe cycling in natural systems (10–13). Here we show that NO_3^- is dominant in the control of both As and Fe cycling during anoxia in urban, seasonally stratified, and eutrophic Upper Mystic Lake (UML; maximum depth ~ 24 m, surface area ~ 50 ha, volume ~ 7×10^6 m³). The results have

implications for element cycles in many N-polluted aquatic systems.

UML's sediments contain 200 to 2100 parts per million (ppm) of As, derived primarily from industrial activity (14). These sediments are a seasonal source of As to the water column (15–17). Conventionally, the presence or absence of O_2 is considered the main determinant of Fe (10) and As (18) chemistry in nonsulfidic lake waters (19), and anoxia does initiate release of Fe and As from UML sediments into the hypolimnion (depths ~ 10 to 24 m). However, the expected reduced chemical forms, As(III) and dissolved Fe(II) (19), have only materialized occasionally in UML (15). Instead, oxidized As and particulate Fe(III) have accumulated in the anoxic water column during most years (16, 17, 20). For example, by late July 1997, O_2 had fallen below detection limits (~5 μM) in waters deeper than 15 m, and Fe and As began to be released from the sediments (Fig. 1, A and B) (21). Fe(II) and As(III), however, represented only small percentages of total As and Fe throughout the following 4 months of anoxia. Because the Fe must have been remobilized from the sediments in soluble form as Fe(II), most of this Fe was oxidized subsequent to release, in the absence of O_2 . Similarly, any As remobilized as As(III) must have been anaerobically oxidized to As(V).

We hypothesized that NO_3^- was responsible for the dominance of oxidized Fe and As. In UML, as in many eutrophic lakes, NO_3^- levels (21) frequently exceed 100 μM (Fig. 2). Persisting for several months after seasonal thermal stratification (thermocline at depth of 7 m) and subsequent O_2 depletion in UML, a large fraction of the NO_3^- pool was produced in situ through microbial oxidation of NH_4^+ (i.e., nitrification).

Parsons Laboratory, Department of Civil and Environmental Engineering, Massachusetts Institute of Technology, Cambridge, MA 02139, USA.

*Present address: Department of Environmental Science and Engineering, Harvard School of Public Health, Building 1 Room G21, 665 Huntington Avenue, Boston, MA 02115, USA.

†To whom correspondence should be addressed. E-mail: dbsenn@alum.mit.edu

REPORTS

Field observations confirm nitrate's control over Fe chemistry in UML. NO_3^- did not become fully depleted in 1997, and as predicted, Fe(II) levels remained low. By contrast, in 1999, NO_3^- depletion occurred in the deepest waters by late October, and resulting Fe(II) accumulation was highly coincident, spatially and temporally, with the NO_3^- -depleted region (Fig. 3A). An HFO peak developed at the NO_3^- -rich/ NO_3^- -depleted interface, analogous to the peak observed at the oxic-anoxic interface in systems in which O_2 controls Fe cycling (19).

Mass balance at depths of 21 to 24 m indicated that NO_3^- , rather than other oxidants, was responsible for oxidizing most Fe(II) during anoxic, NO_3^- -rich periods (21). In 1997, O_2 and $\text{Mn}^{\text{IV}}\text{O}_2$ accounted for at most 25% of Fe(II) oxidation [total Fe(II) oxidation = $60,000 \pm 18,000 \text{ mol} = 60,000 \text{ e}^-$ equivalents), whereas only 40% of the NO_3^- consumption was required (total NO_3^- consumption = $29,000 \text{ mol} = 145,000 \text{ e}^-$ equivalents, assuming N_2 to be the product). The remaining NO_3^- consumption likely occurred through conventional denitrification. Mass balances for

Fe(II) oxidation in 1998 and 1999 yielded similar results (20).

Although abiotic Fe(II) oxidation by NO_3^- proceeds at insignificant rates under conditions typical of UML (22), microcosm experiments using anoxic surface-sediment slurries spiked with NO_3^- (21) demonstrated the feasibility of biologically mediated Fe(II) oxidation by NO_3^- in this system (Fig. 3B). NO_3^- consumption ($\sim 1 \text{ mM}$, or $5 \text{ meq e}^- \text{ liter}^{-1}$ when NO_3^- reduction to N_2 is considered) was sufficient to explain the observed oxidation of both Fe(II) ($1.2 \text{ meq e}^- \text{ liter}^{-1}$) and S(-II) [$2.1 \text{ meq e}^- \text{ liter}^{-1}$ (20)], whereas negligible Fe (or sulfide) oxidation was observed in controls killed with azide or formaldehyde. These observations are consistent with culture-based studies demonstrating the existence of bacteria that can mediate Fe(II) oxidation through reduction of NO_3^- , primarily to N_2 (and some N_2O) (6–8).

The presence or absence of NO_3^- also dictated As redox chemistry (Figs. 1B and 3C). Contrary to conventional expectation (19), As(V), rather than As(III), accumulated during anoxic but NO_3^- -rich periods. In that As is primarily released from anoxic sediments as

As(III) (19), the dominance of As(V) at these times is best explained through As(III) oxidation by NO_3^- [at a pseudo-first order rate of $\sim 0.2 \text{ day}^{-1}$, estimated by mass balance, conservatively assuming that 50% of the As was remobilized as As(III)]. This is consistent with the recent discovery of bacteria that couple As(III) oxidation with NO_3^- reduction (9). Because As occurred at submicromolar concentrations, electron balance arguments alone cannot uniquely identify the oxidant [i.e., levels of $\text{Mn}^{\text{IV}}\text{O}_{2(s)}$ or O_2 slightly below detection limits cannot be eliminated on strict mass balance considerations]. However, the presence of NO_3^- and dominance of As(V) were spatially and temporally coincident throughout summer and fall 1997, summer to mid-fall 1998 (20), and summer to early fall 1999.

By contrast, immediately upon NO_3^- depletion during fall 1999, As(III) concentrations increased rapidly at NO_3^- -depleted depths (Fig. 3C), further supporting the argument that NO_3^- had been the primary As(III) oxidant. An alternative explanation, that NO_3^- had been oxidizing As(III) indirectly through NO_3^- -produced Fe(III) (9), is countered by the fact that much As(III) accumulated during 1999 (Fig. 3, A and C) before all Fe(III) was reduced. Following NO_3^- depletion (October to December 1999), mass balance suggests that both continued release of As(III) from the sediments and reduction of As(V) already in the water column occurred. The latter process could have been inhibited earlier by the presence of NO_3^- or simply masked by concurrent oxidation of As(III) (9).

An important consequence of NO_3^- leading to the dominance of HFO and As(V) is that most As should form particulate HFO-complexes. To confirm this hypothesis, we designed a N_2 -purged in situ serial filtration system to measure size distributions of Fe and As in anoxic water when NO_3^- was present (20). This device rigorously excludes O_2 and filters

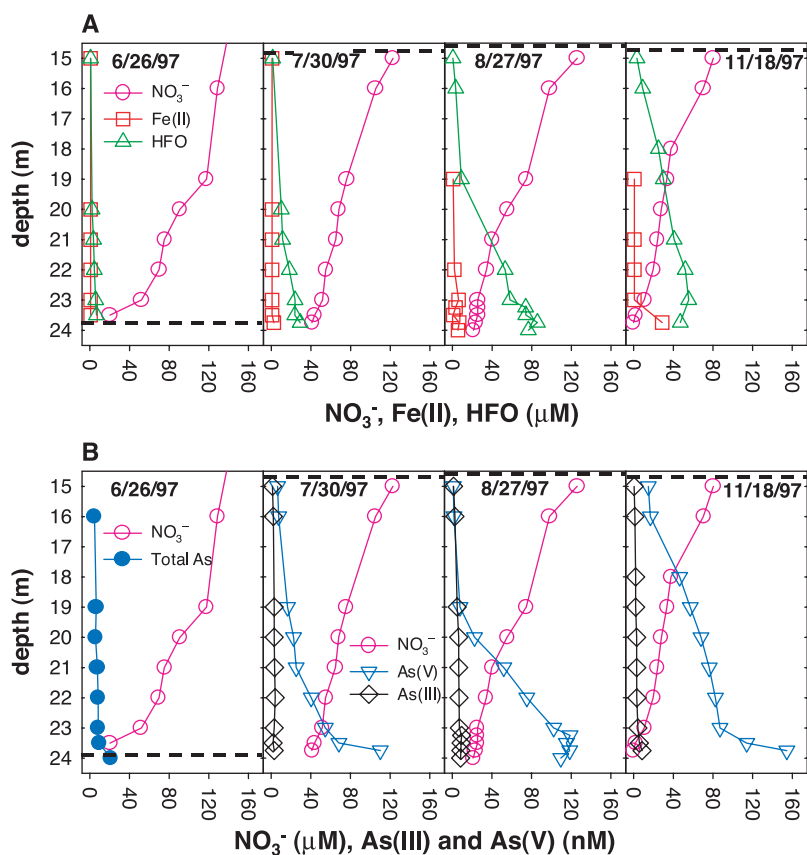


Fig. 1. Observed Fe and As profiles in UML during 1997. Primarily (A) HFO and (B) As(V) accumulated in the hypolimnion under anoxic, NO_3^- -rich conditions, as opposed to the expected Fe(II) and As(III). Elevated Fe(II) was measured within 25 to 50 cm of the sediment-water interface on 8/13/97 (not shown); however, Fe(II) concentrations remained much lower than HFO concentrations, until mid-November in the deepest samples. O_2 concentrations were below detection limits (less than $\sim 5 \mu\text{M}$) in waters deeper than those denoted by the dashed line. HFO was calculated as the difference between total Fe and Fe(II). As(V) was calculated as the difference between total As and As(III).

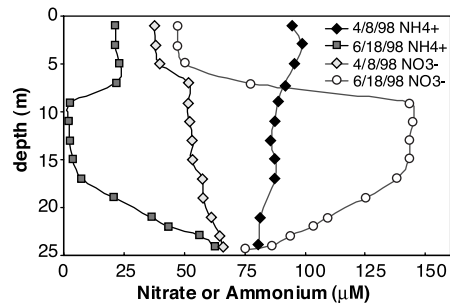


Fig. 2. Spring and early-summer profiles of NO_3^- and NH_4^+ in UML. After spring stratification, much of the hypolimnetic ammonia was nitrified, i.e., $\text{NH}_4^+ + 2\text{O}_2 \rightarrow \text{NO}_3^- + 2\text{H}^+ + \text{H}_2\text{O}$. This increased the hypolimnetic NO_3^- pool by 150%, making NO_3^- the most abundant oxidant. Mass balance estimates indicate that $\sim 45\%$ of hypolimnetic O_2 was consumed by this process during 1998. Similar profiles were observed in 1999.

REPORTS

at low velocities ($\sim 0.02 \text{ cm min}^{-1}$), minimizing possible artefacts such as Fe(II) oxidation and accelerated coagulation. During 1997, $\sim 95\%$ of As was associated with particles (including colloids) at 22 m (representative hypolimnetic depth) throughout the period of anoxia (fig. 1S). Similar observations were made at 20 and 22 m during fall 1996. Using surface complexation modeling (21, 23) of As sorption by HFO, we predicted (typically within $\pm 15\%$) the measured distribution of As between particulate and dissolved (i.e., smaller than $0.05 \mu\text{m}$) phases. Although the presence of other sorbing surfaces cannot be ruled out, none is needed to explain the observations. We calculate that $>90\%$ of As was complexed by HFO in late November 1997 in the bottom 4 m of the lake. Had As been present entirely as As(III), less [only $\sim 60\%$, calculated using sorption constants of (3)] would have been complexed by HFO. Over the entire season, mass balance estimates indicate that settling resulted in a 40%

decrease in net As remobilization to the water column.

N pollution may thus have direct effects on the cycling of As in numerous other systems and may indirectly alter the cycling of other particle-reactive substances (e.g., PO_4^{3-} , Pb, Hg, Cd) through the Fe cycle. These effects may not necessarily be adverse; in some instances, lowered metal toxicity could result owing to sorption by HFO. NO_3^- levels greater than $50 \mu\text{M}$ are common in lakes across the United States and Europe (table S1). Elevated NO_3^- is at least partly responsible for many coastal eutrophic "dead zones" (24) (table S1) and may influence Fe and trace metal geochemistry there. Many groundwaters in the United States contain elevated NO_3^- (25) (table S1). Postma *et al.* (26) provide evidence for oxidation of reduced Fe (as pyrite) in a NO_3^- -contaminated aquifer, and biologically mediated Fe(II) oxidation by NO_3^- has recently been demonstrated in laboratory studies of anoxic paddy soils (27). Elevated NO_3^- has also been measured in some Bangladesh groundwaters (28, 29) (table S1), which commonly contain elevated As. Although these As concentrations are often much greater than those in UML, and multiple solid phases are present, the few available data (i.e., in which both NO_3^- and As have been measured) suggest that As tends to decrease at high NO_3^- levels (28, 29).

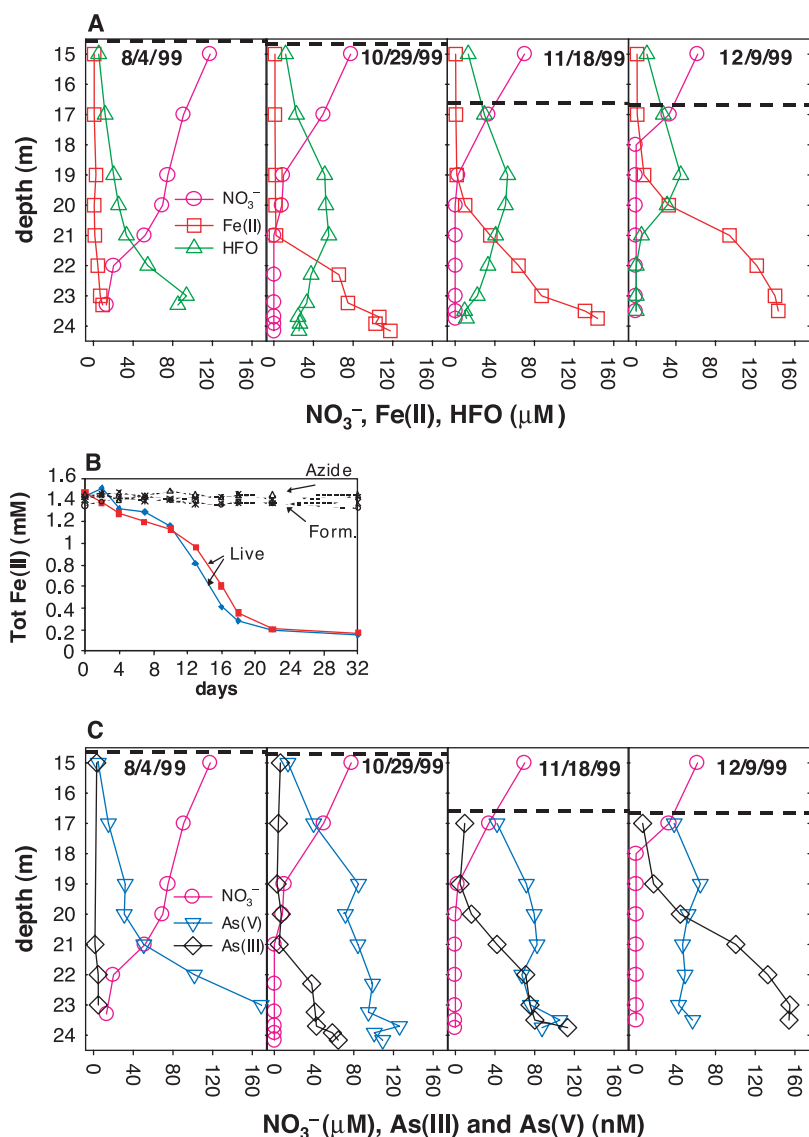


Fig. 3. Impact of NO_3^- on Fe and As redox chemistry. (A) During 1999, particulate HFO initially accumulated in anoxic, NO_3^- -rich waters, but was replaced by dissolved Fe(II) at NO_3^- -depleted depths. (B) Fe(II) oxidation by NO_3^- in anaerobic sediment-slurry. In live bottles, slurry color changed from black to orange-brown as Fe(II) levels decreased, suggesting that Fe(II), likely as $\text{Fe}^{\text{II}}\text{S}_2$, was oxidized to HFOs. The concomitant accumulation of sulfate (data not shown) is consistent with this interpretation. Nitrite (NO_2^-) did occur transiently in live bottles (maximum of 0.2 mM) but decreased to less than 0.01 mM before most Fe(II) oxidation occurred. In addition, NO_2^- was observed in the formaldehyde controls (up to 0.13 mM by day 32) in which no Fe(II) oxidation was observed, suggesting that abiotic Fe(II) oxidation by NO_2^- was not important under these conditions. (C) As(V) accumulated in the water column during summer and early fall of 1999 when NO_3^- was present, but As(III) replaced As(V) at NO_3^- -depleted depths. O_2 concentrations were below detection limits (less than $\sim 5 \mu\text{M}$) in waters deeper than those denoted by the dashed line. HFO was calculated as the difference between total Fe and Fe(II). As(V) was calculated as the difference between total As and As(III).

References and Notes

- W. R. Cullen, K. J. Reimer, *Chem. Rev.* **89**, 713 (1989).
- K. P. Raven, A. Jain, R. H. Loeppert, *Environ. Sci. Technol.* **32**, 344 (1998).
- M. L. Pierce, C. B. Moore, *Water Res.* **16**, 1247 (1982).
- D. E. Cummings, F. Caccavo Jr., S. Fendorf, R. F. Rosenzweig, *Environ. Sci. Technol.* **33**, 723 (1999).
- P. M. Vitousek *et al.*, *Ecol. Appl.* **7**, 737 (1997).
- M. Benz, A. Brune, B. Schink, *Archiv. Microbiol.* **169**, 159 (1998).
- K. L. Straub, M. Benz, B. Schink, F. Widdel, *Appl. Environ. Microbiol.* **62**, 1458 (1996).
- K. A. Weber, F. W. Picardal, E. E. Roden, *Environ. Sci. Technol.* **35**, 1644 (2001).
- S. E. Hoefft, F. Lucas, J. T. Hollibaugh, R. S. Oremland, *Geomicrobiol. J.* **19**, 1 (2002).
- W. Davison, *Earth Sci. Rev.* **34**, 119 (1993).
- D. Postma, C. Boesen, *Water Resour. Res.* **27**, 2027 (1991).
- J. W. Murray, L. A. Codispoti, F. E. Friederich, in *Aquatic Chemistry: Interfacial and Interspecies Processes*, C. P. Huang, C. R. O'Melia, J. J. Morgan, Eds. (American Chemical Society, Washington, DC, 1995), p. 157.
- R. R. DeVitre, J. Buffle, D. Perret, R. Baudat, *Geochim. Cosmochim. Acta* **52**, 1601 (1988).
- H. M. Spliethoff, H. F. Hemond, *Environ. Sci. Technol.* **30**, 121 (1996).
- H. M. Spliethoff, R. P. Mason, H. F. Hemond, *Environ. Sci. Technol.* **29**, 2157 (1995).
- P. R. Trowbridge, thesis, Massachusetts Institute of Technology (1995).
- A. C. Aurilio, R. P. Mason, H. F. Hemond, *Environ. Sci. Technol.* **28**, 577 (1994).
- J. Aggett, M. R. Kriegman, *Water Res.* **4**, 407 (1988).
- Classical Fe and As cycling in lakes: Fe(II) (70) and As(III) (78) are expected to dominate in anoxic waters. In oxic, circumneutral-pH sediments, Fe(III) typically occurs as insoluble and highly sorptive HFO solids, which can be reduced to soluble Fe^{2+} when O_2 is depleted, as commonly happens beneath a lake's thermocline during the summer (70). When this occurs, both Fe(II) and substances previously sorbed by HFO are released from the

sediments to the water column (10). Fe(II) accumulates in the anoxic waters, and upward-diffusing Fe(II) can be quickly oxidized at the anoxic:oxic interface, causing the precipitation of HFO, which can then scavenge As and other particle-reactive compounds and settle. During reductive dissolution of HFO, sorbed As(V) is generally reduced to As(III) (30, 31). This is consistent with thermodynamic predictions in an Fe-reducing system [50 to 98% of As should be present as As(III) at Fe(II) levels from 50 to 100 μM and pH 6.6 to 6.8]. It is therefore As(III), which is typically found to constitute most pore-water As in reducing sediments and soils (18, 32, 33), that should diffuse into overlying anoxic waters. Direct mobilization of As(V) during HFO reduction has only been observed in laboratory pure culture study with an Fe(III)-reducing bacterium (4). At the anoxic:oxic interface, abiotic or biologically mediated (34) As(III) oxidation by O₂ may take place. Abiotic oxidation by particulate Mn(IV)O₂ is also possible (35).

20. D. B. Senn, thesis, Massachusetts Institute of Technology (2001).

21. Materials and methods are available as supporting material on Science Online.

22. C. J. Ottley, W. Davison, W. M. Edmunds, *Geochim. Cosmochim. Acta* **61**, 1819 (1997).

23. D. Dzombak, F. M. M. Morel, *Surface Complexation Modeling: Hydrous Ferric Oxide* (Wiley Interscience, New York, 1990).

24. S. W. A. Naqvi et al., *Nature* **408**, 346 (2000).

25. B. T. Nolan, J. D. Stoner, *Environ. Sci. Technol.* **34**, 1156 (2000).

26. D. Postma, C. Boesen, H. Kristiansen, F. Larsen, *Water Resour. Res.* **27**, 2027 (1991).

27. S. Ratering, S. Schnell, *Environ. Microbiol.* **3**, 100 (2001).

28. British Geological Survey, www.bgs.ac.uk/arsenic/bangladesh/datadownload.htm.

29. R. T. Nickson, J. M. McArthur, P. Ravenscroft, W. G. Burgess, K. M. Ahmed, *Appl. Geochem.* **15**, 403 (2000).

30. D. Ahmann, L. R. Krumholz, H. F. Hemond, D. R. Lovley, F. M. M. Morel, *Environ. Sci. Technol.* **31**, 2923 (1998).

31. J. M. Harrington, S. E. Fendorf, R. F. Rosenzweig, *Environ. Sci. Technol.* **32**, 2425 (1998).

32. P. H. Masscheleyn, R. D. Delaune, W. H. Patrick, *Environ. Sci. Technol.* **25**, 1414 (1991).

33. J. N. Moore, W. H. Ficklin, C. Johns, *Environ. Sci. Technol.* **22**, 432 (1988).

34. J. A. Wilkie, J. G. Hering, *Environ. Sci. Technol.* **32**, 657 (1998).

35. M. J. Scott, J. J. Morgan, *Environ. Sci. Technol.* **29**, 1898 (1995).

36. B. Voelker and P. Gschwend provided guidance throughout the study, D. Ahmann and J. Jay aided in developing microcosm procedures, and D. Brabander assisted with field work. This research was funded by National Institute of Environmental Health Sciences (NIEHS) Superfund Basic Research Program grant 5P42ES04675-06.

Supporting Online Material
www.sciencemag.org/cgi/content/full/296/5577/2373/DC1.
 Materials and Methods
 Fig. S1
 Table S1

1 April 2002; accepted 30 May 2002

50 Million Years of Genomic Stasis in Endosymbiotic Bacteria

Ivica Tamas,^{1*} Lisa Klasson,^{1*} Björn Canbäck,¹

A. Kristina Näslund,¹ Ann-Sofie Eriksson,¹

Jennifer J. Werngreen,² Jonas P. Sandström,¹ Nancy A. Moran,²

Siv G. E. Andersson^{1†}

Comparison of two fully sequenced genomes of *Buchnera aphidicola*, the obligate endosymbionts of aphids, reveals the most extreme genome stability to date: no chromosome rearrangements or gene acquisitions have occurred in the past 50 to 70 million years, despite substantial sequence evolution and the inactivation and loss of individual genes. In contrast, the genomes of their closest free-living relatives, *Escherichia coli* and *Salmonella* spp., are more than 2000-fold more labile in content and gene order. The genomic stasis of *B. aphidicola*, likely attributable to the loss of phages, repeated sequences, and *recA*, indicates that *B. aphidicola* is no longer a source of ecological innovation for its hosts.

The availability of genome sequences for related bacteria is providing exciting insights into evolution, but one limitation has been the lack of identifiable bacterial fossils to provide a time frame for these studies. We have quantified total rates of genomic evolution for *Buchnera aphidicola*, an obligate mutualistic symbiont of aphids, by sequencing the genome of the *B. aphidicola* symbiont of *Schizaphis graminum* (Sg) (1) and analyzing its divergence from the published sequence of the *B. aphidicola* symbiont of *Acyrtosiphon pisum* (Ap) (2).

This case allows genome evolution to be calibrated reliably with respect to time. Because the symbiont phylogeny mirrors that of its aphid hosts, indicating synchronous diversification, divergence dates reconstructed for ances-

tral aphids can be extended to the corresponding *B. aphidicola* ancestors. This approach has been used to infer that this endosymbiosis was established at least 150 million years ago (Ma) and that the lineages represented by *B. aphidicola* (Sg) and *B. aphidicola* (Ap) diverged 50 to 70 Ma (3, 4) (Fig. 1A). These are the only fully sequenced organisms that have eliminated *recA*, which is expected to lower the incidence of recombination events (5).

The genomes of *B. aphidicola* (Sg) and *B. aphidicola* (Ap) are similar in size [0.64 megabases (Mb)] and are among the smallest of

bacterial genomes. Their gene content is also very similar, with 526 genes shared of the 564 and 545 intact genes present in *B. aphidicola* (Ap) and *B. aphidicola* (Sg), respectively (Table 1). A comparison of the aligned genome sequences (1) confirms a high degree of divergence at the nucleotide sequence level. On the basis of a divergence date of 50 million years (My), average rates of sequence evolution were estimated at 9.0×10^{-9} synonymous substitutions per site per year and 1.65×10^{-9} nonsynonymous substitutions per site per year. The observed divergence at synonymous sites shows low variance among genes (1), suggesting that the synonymous divergence level corresponds to the mutation rate of *B. aphidicola*, which is similar to or slightly higher than the rate estimated in *E. coli* and *Salmonella typhimurium* (4, 6, 7).

Despite high levels of sequence divergence, the two *B. aphidicola* genomes show complete conservation of genomic architecture (Fig. 1B). No inversions, translocations, duplications, or gene acquisitions have occurred in either lineage since their divergence. Of the 564 protein-coding genes originally annotated in *B. aphidicola* (Ap), only four (*yba1* to *yba4*) were reported not to have orthologs in *E. coli* (2), a closely related free-living species (Fig. 2A). Our analyses suggest that even these genes were present before the establishment of the symbiosis (1), providing even stronger evidence that the symbiotic life-style did not in-

Table 1. Comparison of genome features for *B. aphidicola* (Sg) and *B. aphidicola* (Ap).

Feature	<i>B. aphidicola</i> (Sg)	<i>B. aphidicola</i> (Ap)
Genome size (bp)	641,454	640,681
Genic G + C content (%)	26.2	26.3
Intergenic G + C content (%)	14.8	16.1
Protein coding genes (no.)	545	564
Pseudogenes (no.)	38	13
Avg. gene length (bp)	978	985
Avg. intergenic length (bp)	118	127

¹Department of Molecular Evolution, Evolutionary Biology Center, University of Uppsala, Uppsala, Sweden.

²Department of Ecology and Evolutionary Biology, University of Arizona, Tucson, AZ 85721, USA.

*These authors contributed equally to this work.

†To whom correspondence should be addressed. E-mail: Siv.Andersson@ebc.uu.se